IJRCS

International Journal of Robotics and Control Systems
Vol. 6, No. 2, 2026, pp. 1573-1592
ISSN 2775-2658
http://pubs2.ascee.org/index.php/ijrcs

ASCEE

RISE-Based Actor–Critic Control for a Four-Wheeled Mecanum Robot with Center-of-Mass Offset

Minh Dong Nguyen [a,1], Hai Binh Nguyen [b,2,*]

[a] Faculty of Electronics and Telecommunications, Electric Power University, Hanoi, Vietnam
[b] Faculty of Electrical - Automation, University of Economics Technology for Industrial, Hanoi, Vietnam
[1] dongnm@epu.edu.vn; [2] nhbinh@uneti.edu.vn
[*] Corresponding Author

ARTICLE INFO

Article History
Received February 20, 2026
Revised March 25, 2026
Accepted May 12, 2026

Keywords
Reinforcement Learning;
Actor–Critic;
Robust Integral of the Sign of the Error (RISE);
Four-Wheeled Mecanum Robot;
Trajectory Tracking

ABSTRACT

This paper presents a RISE-based Actor–Critic control scheme for a four-wheeled Mecanum mobile robot subject to manipulator-induced center-of-mass (COM) offset and dynamic uncertainties. The COM deviation is explicitly modeled, leading to nonuniform wheel loading and wheel-dependent slipping. By transforming the time-varying tracking problem into an autonomous affine system, an online Actor–Critic algorithm with a discounted cost function is developed to achieve optimal trajectory tracking. A multi-channel RISE feedback term is integrated to compensate COM-induced and slip-related disturbances without requiring persistent excitation. Lyapunov analysis guarantees uniformly ultimately bounded closed-loop behavior, and simulation results demonstrate improved tracking accuracy and robustness under time-varying COM offsets.

© 2025 The Authors.
Published by Association for Scientific Computing Electrical and Engineering.
This is an open access article under the CC-BY-SA license.

1. Introduction

Four-wheeled Mecanum wheeled mobile robots (FMWRs) have been widely adopted in modern robotic applications due to their omnidirectional mobility, compact mechanical structure, and superior maneuverability in confined environments. These advantages make FMWRs particularly attractive for logistics automation, service robotics, industrial transportation, and intelligent warehousing systems [1], [2], [6]–[8]. In recent years, FMWRs have increasingly served as mobile platforms for robotic manipulators, forming so-called mobile manipulator systems that integrate locomotion and manipulation capabilities to execute complex tasks in unstructured environments [3], [4], [9]–[11].

The integration of a robotic arm onto a Mecanum mobile base introduces a time-varying center-of-mass (COM) shift, which changes the wheel load distribution and alters the dynamic behavior of the platform. For wheeled mobile manipulators, such dynamic coupling between the manipulator and the mobile base is a well-known challenge because it can degrade motion stability and tracking accuracy [5], [12], [13]. Therefore, explicitly accounting for COM offset is important for reliable trajectory tracking of Mecanum mobile manipulators.

The presence of COM offset leads to an unbalanced normal force distribution among Mecanum wheels, directly affecting the wheel-ground interaction and the traction capability. Previous studies have shown that variations in normal forces can severely influence the dynamic behavior of wheeled robots, resulting in asymmetric actuation effectiveness and increased sensitivity to disturbances [14]–

[17], [20], [21]. For Mecanum-wheeled systems, this issue is further amplified by the roller-based wheel design, which inherently introduces additional slip components. Consequently, COM-induced load redistribution often gives rise to wheel-dependent slipping, where each wheel experiences distinct and time-varying slip characteristics [22]. Such effects may cause oscillatory motion, trajectory deviation, or even instability, particularly when the manipulator and mobile base move simultaneously. A comprehensive dynamic model explicitly accounting for center-of-mass offset and frictional uncertainties was developed in [18], while an integrated mathematical model that jointly captures both the dynamic and kinematic characteristics of the system was analyzed and validated in [19]

A considerable body of literature has addressed trajectory tracking control of Mecanum-wheeled mobile robots using kinematic control, feedback linearization, and nonlinear Lyapunov-based methods [19], [23]–[25], [37]. Although these approaches can achieve satisfactory performance under ideal assumptions, most of them rely on simplified dynamic models that assume a centrally located COM and neglect the coupling effects introduced by mass redistribution. Robust control techniques, including sliding mode control and adaptive control, have been proposed to mitigate modeling uncertainties and external disturbances [26], [27], [39], [46]–[49]. However, such methods often require conservative gain tuning, suffer from chattering, or depend on prior knowledge of uncertainty bounds, which limits their applicability to mobile manipulators with rapidly varying COM.

In parallel, reinforcement learning (RL) has emerged as a powerful framework for optimal control of nonlinear robotic systems. Actor–Critic reinforcement learning architectures have been successfully applied to mobile robots and autonomous systems to achieve optimal trajectory tracking without explicitly solving the Hamilton-Jacobi-Bellman (HJB) equations [28], [29], [40]–[43], [50]–[54]. Nevertheless, most existing RL-based control schemes either assume accurate dynamic models or treat complex physical effects, such as COM offset and wheel slip, as lumped disturbances. Moreover, many RL algorithms require the persistent excitation (PE) condition to guarantee convergence of learning parameters, which is difficult to ensure in practical mobile manipulation tasks where motion patterns are task-driven and repetitive [30].

On the other hand, the Robust Integral of the Sign of the Error (RISE) technique has been demonstrated as an effective approach for compensating unmodeled dynamics and time-varying disturbances in nonlinear systems [31]–[35]. RISE-based controllers offer strong robustness properties and can achieve asymptotic or uniformly ultimately bounded tracking performance without requiring PE conditions. These features make RISE particularly suitable for robotic systems subject to COM-induced disturbances and load variations. However, existing RISE-based methods primarily focus on stability and robustness, while optimality considerations are rarely incorporated, especially in the context of FMWRs with manipulator-induced COM offset.

Actor–Critic reinforcement learning has become an effective framework for continuous-time nonlinear control because it can approximate the solution of the Hamilton–Jacobi–Bellman equation online and generate an implementable feedback policy without requiring an explicit analytical solution [55]–[57]. However, when the controlled system is subject to time-varying uncertainties, model mismatch, and disturbance-contaminated measurements, purely RL-based schemes may suffer from degraded learning performance and limited robustness in practical robotic applications. In contrast, the robust integral of the sign of the error (RISE) methodology has demonstrated strong disturbance-rejection capability and favorable tracking properties for uncertain nonlinear systems [58]–[62].

Therefore, combining Actor–Critic learning with a RISE compensation mechanism provides a meaningful hybrid structure, in which the learning component improves tracking performance while the RISE term enhances robustness against slip-related disturbances and other unmodeled effects. This motivation is particularly relevant for Mecanum mobile robots operating under payload variation and center-of-mass offset, where both performance optimization and disturbance attenuation are required. Motivated by the above observations, this paper proposes a RISE-based Actor–Critic reinforcement

learning controller for a four-wheeled Mecanum mobile robot under center-of-mass offset and wheel-dependent slipping. The trajectory-tracking problem is reformulated into an autonomous affine system, where an online Actor–Critic scheme improves tracking performance and a RISE term compensates for COM-induced and slip-related disturbances.

The main contributions of this paper are summarized as follows:

A RISE-based Actor–Critic reinforcement learning controller with a discount factor is proposed to achieve optimal and robust trajectory tracking under COM-induced dynamic uncertainties. A rigorous Lyapunov-based stability analysis is provided, guaranteeing uniformly ultimately bounded closed-loop behavior and disturbance estimation convergence without the persistent excitation condition.

The remainder of this paper is organized as follows. Section 2 presents the kinematic and dynamic modeling of the FMWR with center-of-mass offset. Section 3 describes the proposed RISE-based Actor–Critic reinforcement learning controller. Stability analysis is provided in Section 4, followed by simulation results in Section 5. Conclusions and future research.

2. Dynamic Modeling of the Four-Wheeled Mecanum Mobile Robot with Center-of-Mass Offset

Consider a four-wheeled Mecanum mobile robot (FMWR) operating on a planar surface and equipped with a robotic manipulator, as illustrated in Fig. 1. An inertial reference frame $\{O_I, X_I, Y_I\}$ is defined on the ground, while a body-fixed reference frame $\{O_R, X_R, Y_R\}$ is attached to the geometric center O_R of the mobile base.

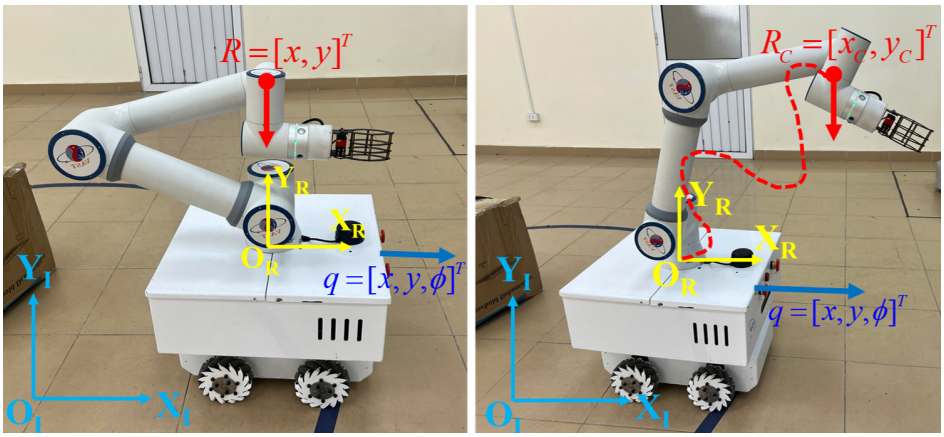

Fig. 1. Experimental four-wheeled Mecanum mobile manipulator under different COM conditions (a), (b)

The generalized coordinate vector of the robot is defined as

$$\mathbf{q} = [x \; y \; \phi]^T \tag{1}$$

Where x and y denote the position of the mobile base in the inertial frame, and ϕ represents the orientation of the robot.

As shown in Fig. 1(a), when the robotic manipulator remains in a compact and symmetric configuration, the overall center of mass (COM) of the system is located close to the geometric center O_R. Under this condition, the mass distribution of the FMWR can be regarded as approximately balanced, and conventional dynamic models assuming a centralized COM provide a reasonable approximation [14]–[17]. However, when the manipulator moves away from the base, as illustrated in Fig. 1(b), the mass distribution of the system becomes asymmetric, resulting in a shifted and time-varying COM.

To explicitly capture this effect, the actual COM location R_c is defined relative to the body-fixed frame $\{O_R, X_R, Y_R\}$, as depicted in Fig. 1(b). The COM offset vector is defined as

$$\mathbf{R}_c = \begin{bmatrix} r_x \\ r_y \end{bmatrix}, \tag{2}$$

Where r_x and r_y denote the longitudinal and lateral displacement of the COM with respect to the geometric center O_R, respectively. The vector $\mathbf{R}_c$ is generally time-varying and depends on the configuration and motion of the mounted manipulator. To ensure static stability and prevent rollover, the COM offset is assumed to be bounded as

$$|r_x| < L, \qquad |r_y| < W, \tag{3}$$

Where L and W are positive constants determined by the geometric stability margin of the robot platform. This assumption guarantees that the projection of the COM remains inside the support polygon during motion, thereby reducing the risk of rollover when the manipulator induces a time-varying mass eccentricity.

As illustrated in Fig. 2, the presence of the COM offset introduces an eccentric mass distribution, which leads to coupling between the translational and rotational dynamics of the mobile base.

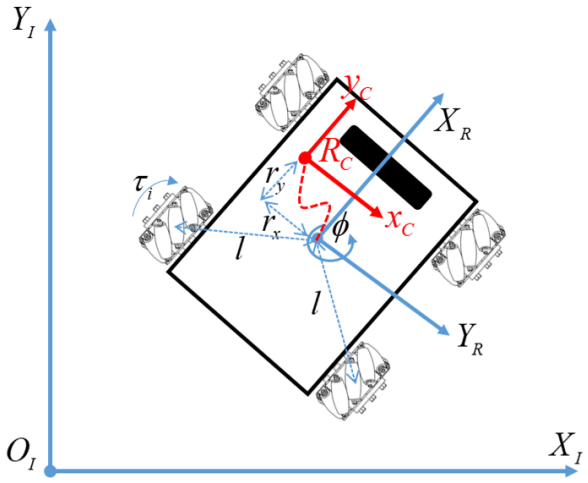

Fig. 2. Dynamic modeling of the four-wheeled Mecanum mobile robot with time-varying center-of-mass offset, showing the inertial frame $\{O_I, X_I, Y_I\}$, the body-fixed frame $\{O_R, X_R, Y_R\}$, wheel configuration, and the COM displacement vector $\mathbf{R}_c = [r_x, r_y]^T$ resulting from manipulator motion

Moreover, the normal forces acting on the individual Mecanum wheels become nonuniform, resulting in wheel-dependent friction forces and slipping phenomena. These effects introduce additional dynamic uncertainties that cannot be adequately described by conventional FMWR models assuming a fixed and centralized COM.

By explicitly incorporating the COM offset, the planar dynamic equations of the FMWR can be expressed in the following compact form [36], [38]:

$$\mathbf{M}(\mathbf{R}_c)\ddot{\mathbf{q}} + \mathbf{C}(\mathbf{q}, \dot{\mathbf{q}}, \mathbf{R}_c)\dot{\mathbf{q}} + \mathbf{D}(\mathbf{R}_c, \boldsymbol{\rho}) = \mathbf{B}\boldsymbol{\tau}, \tag{4}$$

Where $\mathbf{M}(\mathbf{R}_c) \in \mathbb{R}^{3\times3}$ denotes the inertia matrix modified by the COM offset:

$$\begin{aligned}
m_{11} &= m_b + 4\left(m_w + \tfrac{I}{r^2}\right); \\
m_{22} &= m_b + 4\left(m_w + \tfrac{I}{r^2}\right); m_{12} = m_{21} = 0; \\
m_{13} &= m_{31} = m_b\left(r_x \sin\phi + r_y \cos\phi\right); \\
m_{23} &= m_{32} = m_b\left(-r_x \cos\phi + r_y \sin\phi\right) \\
m_{33} &= m_b\left(r_x^2 + r_y^2\right) + I_b + 8\left(m_w + \tfrac{I}{r^2}\right) l^2 \sin^2(\pi/4 - \alpha)
\end{aligned}$$

Where m_b and I_b denote the mass and moment of inertia of the robot body, m_w and I represent the mass and inertia of each wheel, l is the distance from the robot center to each wheel, and α is the roller angle of the Mecanum wheel.

$\mathbf{C}(\cdot)$ represents the Coriolis and centrifugal terms affected by the eccentric mass distribution

$$\mathbf{C} = \begin{bmatrix} 0 & 0 & 0 \\ 0 & 0 & 0 \\ m_b\dot{\phi}(r_x\cos\phi - r_y\sin\phi) & m_b\dot{\phi}(r_x\sin\phi + r_y\cos\phi) & 0 \end{bmatrix}^T \tag{5}$$

The vector $\boldsymbol{\tau}$ represents the wheel torque inputs, $\mathbf{B}$ is the input transformation matrix, and $\boldsymbol{\rho}$ denotes the wheel-dependent slip ratios and $\mathbf{D}(\cdot)$ denotes a lumped disturbance term accounting for COM-induced dynamic coupling and wheel–ground interaction uncertainties.

$$\mathbf{B} = \frac{1}{r}\begin{bmatrix} -(\mathrm{C}\phi - \mathrm{S}\phi) & -(\mathrm{S}\phi + \mathrm{C}\phi) & -\sqrt{2}l\mathrm{S}(\frac{\pi}{4} - \alpha) \\ -(\mathrm{C}\phi + \mathrm{S}\phi) & -(\mathrm{S}\phi - \mathrm{C}\phi) & -\sqrt{2}l\mathrm{S}(\frac{\pi}{4} - \alpha) \\ \mathrm{C}\phi - \mathrm{S}\phi & \mathrm{S}\phi + \mathrm{C}\phi & -\sqrt{2}l\mathrm{S}(\frac{\pi}{4} - \alpha) \\ \mathrm{C}\phi + \mathrm{S}\phi & \mathrm{S}\phi - \mathrm{C}\phi & -\sqrt{2}l\mathrm{S}(\frac{\pi}{4} - \alpha) \end{bmatrix}^T \tag{6}$$

$C\ \phi = \cos\phi; S\phi = \sin\phi$

It is worth noting that when the COM offset satisfies $\mathbf{R}_c = \mathbf{0}$, the dynamic model in (4) reduces to the conventional FMWR dynamics reported in [14]–[17]. Therefore, the proposed formulation can be viewed as a generalized dynamic model that encompasses both balanced configurations, as shown in Fig. 1(a), and unbalanced configurations induced by manipulator motion, as shown in Fig. 1(b). In this work, the COM-induced coupling effects and wheel slipping phenomena are treated as bounded disturbances and will be explicitly compensated through the proposed RISE-based Actor–Critic reinforcement learning control framework.

3. Controller Design

This section presents the control design for the four-wheeled Mecanum mobile robot (FMWR) subject to center-of-mass (COM) offset and dynamic uncertainties. Based on the control-oriented dynamic model derived in Section 2.2, a RISE-based robust controller augmented with an Actor–Critic reinforcement learning (RL) framework is developed to ensure stable trajectory tracking in the presence of time-varying disturbances.

3.1. Control Objective and Problem Formulation

Based on the kinematic model of the four-wheeled Mecanum mobile robot (FMWR), the transformation between the inertial-frame velocity and the body-fixed velocity can be expressed as:

$$v_q = H(\phi)\dot{q} \tag{7}$$

Where

$$H(\phi) = \begin{bmatrix} \cos\phi & \sin\phi & 0 \\ -\sin\phi & \cos\phi & 0 \\ 0 & 0 & 1 \end{bmatrix} \tag{8}$$

Taking the time derivative of (7) yields

$$\dot{v}_q = H(\phi)\ddot{q} + \dot{\phi}\dot{H}(\phi)\dot{q} \tag{9}$$

From the dynamic model of the FMWR derived in the previous section, the generalized acceleration can be expressed as

$$\ddot{q} = M^{-1}B^T\tau - M^{-1}B^T\xi - M^{-1}C\dot{q} \tag{10}$$

Substituting (10) into equation (9), it obtains that:

$$\begin{aligned}\dot{v}_q = & H(\phi)M^{-1}B^T\tau - H(\phi)M^{-1}B^T\xi \\ & - H(\phi)H(\phi)^{-1}M^{-1}Cv_q \\ & + \dot{\phi}\,\dot{H}(\phi)H(\phi)^{-1}v_q\end{aligned} \tag{11}$$

By regrouping terms, the nonlinear dynamics of the FMWR can be rewritten in an affine form with respect to the control input as:

$$\dot{v}_q = \bar{f}(q)v_q + \bar{g}(q)\tau + \bar{g}(q)d(q, v_q) \tag{12}$$

Where

$$\bar{f}(q) = \left[\dot{\phi}\dot{H}(\phi)H(\phi)^{-1} - M^{-1}C\right]$$

$$\bar{g}(q) = H(\phi)M^{-1}B^T$$

$$fd(q, v_q) = -H(\phi)M^{-1}B^T\xi$$

The problem of controlling a robot to follow a set trajectory $q_r(t)$ in a short time with a low cost function. The dynamic model (12) is rewritten as:

$$\dot{x} = f(x) + g(x)\tau + g(x)d\,(q, v_q) \tag{13}$$

Where

$$\begin{aligned}&x = (q^T, v_q^T)^T, \\ &f(x) = (v_q^T, (f(q)v_q)^T)^T, \\ &g(x) = (\mathbf{0}_{3\times 3}, g(q)^T)^T\end{aligned} \tag{14}$$

The control objective is to drive the robot to track a desired reference trajectory $q_r(t)$ while compensating for uncertainties induced by the center-of-mass displacement. To enable reinforcement learning design for time-invariant systems, a reference system is introduced as

$$\dot{x}_r = h_r(x_r) \tag{15}$$

We defining the tracking error as $e = x - x_r$

$$\begin{aligned}\dot{e} &= f(x) + g(x)\tau - h_r(x_r) \\ &= f(x) - h_r(x_r) + g(x)\tau + g(x)u\end{aligned} \tag{16}$$

Where $u = \tau - \tau_r$,

$$\tau_r(x_r) = g^+(x_r)(h_r(x_r) - f(x_r)) \tag{17}$$

By introducing a concatenated state vector $z = (e^T, x_r^T)^T$, then the dynamics of z is formulated by an invariant-time system as

$$\dot{z} = F(z) + G(z)(\hat{u}_{rl} + \tilde{\Delta}) \tag{18}$$

Where

$$F(z) = \begin{pmatrix} f(x) - h_r(x_r) + g(x)\tau_r \\ h_r(x_r) \end{pmatrix}, G(z) = \begin{pmatrix} g(x) \\ \mathbf{0}_{6\times 4} \end{pmatrix}$$

3.2. RISE-Based Online Actor–Critic Control With Discount Factor Under Center-of-Mass Offset

Due to the presence of RISE, dynamic uncertainties or disturbances can be handled by estimating its effects on the, means the error $\tilde{\Delta}$ would be converged to 0. In this section, the nominal system (15) obtained from the perturbed system (14) by ignoring the term $\tilde{\Delta}$ is taken into account in optimal control design.

The input disturbance estimation equation is designed within the RISE framework to robustly estimate and compensate for unknown input disturbances arising from center-of-mass offset variations and modeling uncertainties [44]:

$$\chi(t) = (k_s + 1)\big(e_2(t) - e_2(0)\big) + \int_0^t \Big((k_s + 1)\lambda_2 e_2(\tau) + \beta_1 \operatorname{sgn}\big(e_2(\tau)\big)\Big)\, d\tau \tag{19}$$

The objective of the infinite-horizon optimal control problem is to determine an optimal control scheme $u^*(X)$ that simultaneously achieves the desired tracking performance and minimizes the following cost function with a positive discount factor $\lambda > 0$:

$$V\big(z(t), \hat{u}_r(t)\big) = \int_t^\infty e^{-\lambda(s-t)} U\big(X(s), \hat{u}_r(s)\big)\, ds \tag{20}$$

The instantaneous utility function is defined as

$$U(x, \hat{u}_{rl}) \triangleq x^T \bar{Q} x + \hat{u}_{rl}^T R \hat{u}_{rl}, \tag{21}$$

Where $R \in \mathbb{R}^{n\times n}$ is a symmetric positive definite constant matrix, and $\bar{Q}$ is defined as

$$\bar{Q} = \begin{bmatrix} Q & \mathbf{0}_{2n\times 2n} \\ \mathbf{0}_{2n\times 2n} & \mathbf{0}_{2n\times 2n} \end{bmatrix}. \tag{22}$$

Here, $\bar{Q} \in \mathbb{R}^{2n\times 2n}$ is a positive definite matrix that regulates the weighting of the state vector x. The introduction of the discount factor λ into the performance index ensures the boundedness of the control signal $\hat{u}_{rl}$ as time approaches infinity. By augmenting the state vector as

$$x = \begin{bmatrix} z^T & \eta_d^T & \dot{\eta}_d^T \end{bmatrix}^T \in \mathbb{R}^{4n}, \tag{23}$$

The challenge of developing reinforcement learning algorithms for time-varying systems is addressed. Consequently, the Bellman equation at an arbitrary time instant t can be expressed in terms of the optimal value function $V^*(x(t))$ as

$$V^*(x(t)) = \min_{\hat{u}_{rl}(X(t))\in Y(U)} V\big(x(t), \hat{u}_{rl}(x(t))\big). \tag{24}$$

The discounted Hamiltonian function is derived by taking the time derivative of the Bellman equation using two different approaches. First, a direct derivation yields

$$\frac{d}{dt}V^*(x(t)) = \frac{\partial V^*}{\partial x}\frac{dx}{dt} = \frac{\partial V^*}{\partial x}\big(F(x) + G(x)u^*\big). \tag{25}$$

The second approach is to employ the dynamic programming (DP) principle to evaluate the Bellman equation (24) over an infinitesimal time interval, which yields the following expression:

$$\begin{aligned} V^*(x(t)) = &\int_t^{t+\Delta} e^{-\lambda(s-t)} U\big(x(s), u^*(x(s))\big)\, ds \\ &+ e^{-\lambda\Delta} V^*(x(t+\Delta)). \end{aligned} \tag{26}$$

Accordingly, the following relation can be obtained:

$$\delta_V(t) \triangleq \frac{V^*(x(t)) - V^*(x(t+\Delta))}{\Delta} \tag{27}$$

$$\mathcal{U}_\Delta(t) \triangleq \frac{1}{\Delta}\int_t^{t+\Delta} e^{-\lambda(s-t)} U\big(x(s), u^*(x(s))\big)\, ds \tag{28}$$

$$\mathcal{U}_\Delta(t) \triangleq \frac{1}{\Delta}\int_t^{t+\Delta} e^{-\lambda(s-t)} U\big(x(s), u^*(x(s))\big)\, ds \tag{29}$$

$$\mathcal{D}_\Delta(t) \triangleq \frac{e^{-\lambda\Delta}-1}{\Delta} V^*(x(t+\Delta)) \tag{30}$$

$$\delta_V(t) = \mathcal{U}_\Delta(t) + \mathcal{D}_\Delta(t) \tag{31}$$

In practice, the optimal value function $V^*(x)$ is unknown. Therefore, the Bellman difference $\delta_V(t)$ is approximated onlineand used to construct the critic learning law.

When the time interval approaches an infinitesimal value, i.e., $\Delta \to 0$, the infinite-horizon optimal control problem can be solved recursively at each instant. Under this condition, the control policy is continuously updated such that the optimal value function $V^*(x(t))$ is generated by the corresponding optimal control input $u^*(t)$. Consequently, the discounted Hamilton–Jacobi–Bellman(HJB) equation is obtained as

$$U(x(t), u^*(t)) - \lambda V^*(x(t)) + \frac{\partial V^*}{\partial x}\big(F(x) + G(x)u^*\big) = 0 \tag{32}$$

To explicitly derive the control policy from the value function, an inverse mapping from the optimal value function $V^*(x(t))$ to the optimal control input $u^*(t)$ is formulated using the dynamic programming (DP) principle. Specifically, the optimal value function is expressed as

$$\begin{aligned} V^*(x(t)) = \min_{\hat{u}_r(t)\in Y(U)} \Bigg(& \int_t^{t+\Delta} U(x, \hat{u}_r)\, ds \\ & + e^{-\lambda\Delta} V^*(x(t+\Delta)) \Bigg) \end{aligned} \tag{33}$$

By letting $\Delta \to 0^+$, the above DP formulation leads to an equivalent instantaneous optimal control problem, which provides the inverse relationship between $V^*(x(t))$ and $u^*(t)$ as

$$\begin{aligned} \min_{\hat{u}_r(t)\in Y(U)} \Big(& U(x, \hat{u}_r) - \lambda V^*(x) \\ & + \frac{\partial V^*}{\partial x}\big(F(x) + G(x)\hat{u}_r\big) \Big) = 0 \end{aligned} \tag{34}$$

To facilitate the derivation of the optimal control law, a modified Hamiltonian function incorporating the discount factor $\lambda > 0$ is defined as

$$\begin{aligned} H(x, \hat{u}_r, \nabla V^*, V^*) = {} & x^T Q x + \hat{u}_r^T(x) R \hat{u}_r(x) \\ & - \lambda V^*(x) + \nabla V^{*T}(x)\big(F(x) \\ & + G(x)\hat{u}_r(x)\big) \end{aligned} \tag{35}$$

Where

$$\nabla V^*(x) \triangleq \frac{\partial V^*(x)^T}{\partial x}. \tag{36}$$

Based on the optimality condition implied by (34) and the Hamiltonian defined in (35), the optimal control input $u^*(x)$ can be explicitly derived as

$$\begin{aligned} u^*(x) &= \arg \min_{\hat{u}_r(x) \in Y(\Omega)} \left[H(x, \hat{u}_r, \nabla V^*, V^*) \right] \\ &= -\frac{1}{2} R^{-1} G^T(x) \nabla V^*(x) \end{aligned} \tag{37}$$

Furthermore, by substituting the optimal control policy (37) into the Hamiltonian function and invoking the necessary condition for optimality, and optimization problem (34), the corresponding partial differential equation (PDE) governing the optimal value function is obtained as

$$\begin{aligned} H^*(x, \hat{u}_r, \nabla V^*, V^*) = x^T Q x - \lambda V^*(x) \\ - \frac{1}{4} \nabla V^{*T}(x) G(x) R^{-1} G^T(x) \nabla V^*(x) \\ + \nabla V^{*T}(x) F(x) = 0 \end{aligned} \tag{38}$$

However, it is impossible to analytically solve the partial derivative (38). Therefore, the on-policy actor–critic strategy is employed to seek the optimal control signal in Section 3.3.

3.3. Implementation of an Online Actor–Critic Algorithm

In this subsection, the implementation of the proposed online actor–critic (AC) reinforcement learning algorithm with a discount factor is presented. Due to the presence of center-of-mass (COM) offset–induced uncertainties and the nonlinear nature of the system dynamics, the Hamilton–Jacobi–Bellman (HJB) equation given in (38). Based on the Weierstrass approximation theorem for higher-order functions [43], the optimal value function $V^*(z)$ can be approximated by a single-layer neural network as

$$V^*(z) = W^T \Psi(z) + \varepsilon_v(z), \tag{39}$$

Where $W \in \mathbb{R}^N$ denotes the ideal constant weight vector satisfying $\|W\| \leq \bar{W}$, with $\bar{W}$ being a known positive constant. The vector $\Psi(X) \in \mathbb{R}^N$ represents the activation functions, N is the number of neurons, and $\varepsilon_v(X)$ denotes the function approximation error.

Taking the gradient of (39) with respect to X yields

$$\nabla V^*(z) = \nabla \Psi^T(z) W + \nabla \varepsilon_v(z). \tag{40}$$

It is well established that, over a compact set Ω, both the approximation error $\varepsilon_v(X)$ and its gradient $\nabla \varepsilon_v(X)$ are bounded, i.e., $\|\varepsilon_v\| \leq b_\varepsilon$ and $\|\nabla \varepsilon_v\| \leq b_{\varepsilon x}$ [43]. To facilitate the subsequent stability analysis in Section 3.3, the following assumption regarding the activation functions is introduced.

The activation functions $\Psi(X)$ and their gradients are bounded such that

$$\|\Psi(z)\| \leq b_\psi, \quad \|\nabla \Psi(z)\| \leq b_{\psi x}.$$

Accordingly, the optimal control law in (41) can be reformulated as

$$u^*(z) = -\frac{1}{2} R^{-1} G^T(z) \left(\left(\frac{\partial \Psi}{\partial z} \right)^T W + \left(\frac{\partial \varepsilon_v}{\partial z} \right)^T \right). \tag{41}$$

As the number of neurons N approaches infinity, the approximation errors ε_v and $\nabla \varepsilon_v$ asymptotically converge to zero. For a practical implementation with a finite number of neurons $N \in \mathbb{N}$, the estimated value function and the corresponding control policy are defined as

$$\hat{V}(z, \hat{W}_c) = \hat{W}_c^T \Psi(X), \tag{42}$$

$$\hat{u}_{rl}(X,\hat{W}_a) = -\frac{1}{2}R^{-1}G^T(z)\left(\frac{\partial\Psi}{\partial X}\right)^T\hat{W}_a. \tag{43}$$

Where $\hat{W}_c$ and $\hat{W}_a$ a are the estimates.

The signal control is determined as follows: (17), the tracking controller τ of FWMR can be obtained as

$$\tau = -\frac{1}{2}R^{-1}G^T(z) \bigtriangledown \phi^T(z)\hat{W}_a + g^+(x_r)(h_r(x_r) - f(x_r)) \tag{44}$$

Using the approximations $\hat{u}$ and $\hat{V}$:

$$\begin{aligned}\hat{H}(z,\hat{W}_c,\hat{W}_a) &= \lambda_M^2(z) + z^T\bar{Q}z + \frac{1}{4}\hat{W}_a^T D_1\hat{W}_a \\ -\gamma\hat{W}_c^T\phi + \hat{W}_c^T &\bigtriangledown \phi(F - \frac{1}{2}GR^{-1}G^T \bigtriangledown \phi^T\hat{W}_a)\end{aligned} \tag{45}$$

Define the Bellman error as $\delta = \hat{H} - H^*$,

$$\delta(z,\hat{W}_c,\hat{W}_a) = \lambda_M^2(z) + z^T\bar{Q}z + \frac{1}{4}\hat{W}_a^T D_1\hat{W}_a + \ + \hat{W}_c^T(\bigtriangledown\phi(F + G\hat{u}) - \gamma\phi) \tag{46}$$

Training critic NN to minimize the integral error, The tuning law for the actor NN is developed as

$$\dot{\hat{W}}_a = -\eta_{a1}(\hat{W}_a - \hat{W}_c) - \eta_{a2}\hat{W}_a + \frac{\eta_a}{4}D_1\hat{W}_a\frac{\bar{\sigma}^T}{m_\sigma}\hat{W}_c \tag{47}$$

Where $\eta_{a1} > 0$, $\eta_{a2} > 0$ and $\eta_a > 0$ are tuning parameters.

3.4. Stability Analysis

Considering the candidate Lyapunov function for the stability of the system

$$V(t) = V^*(t) + \frac{1}{2\eta_c}\tilde{W}_c^T(t)\Gamma^{-1}(t)\tilde{W}_c(t) + \frac{1}{2\eta_a}\tilde{W}_a^T(t)\tilde{W}_a(t) \tag{48}$$

In which the optimal cost function has the following derivative:

$$\begin{aligned}\dot{V}^*(t) &= W^T \bigtriangledown \phi F - \frac{1}{2}W^T D_1\hat{W}_a \\ + \bigtriangledown \varepsilon_v^T &\left(F - \frac{1}{2}GR^{-1}G^T \bigtriangledown \phi^T\hat{W}_a\right)\end{aligned} \tag{49}$$

From the HJB equation (38), we can rewrite the optimal cost function determined can be rewritten as:

$$\begin{aligned}\dot{V}^*(t) = -\lambda_M^2(z) - z^T\bar{Q}z + \gamma W^T\phi + \frac{1}{4}W^T D_1 W \\ + \frac{1}{2}\tilde{W}_a^T D_1 W + \frac{1}{2}\tilde{W}_a^T \bigtriangledown \phi D_2 \bigtriangledown \varepsilon_v \\ + \frac{1}{4} \bigtriangledown \varepsilon_v^T D_2 \bigtriangledown \varepsilon_v + \gamma\varepsilon_v(z)\end{aligned} \tag{50}$$

into the derivative of $V(t)$ yields

$$\begin{aligned}\dot{V}(t) = -\lambda_M^2(z) - e^T Qe - \frac{1}{4}W^T D_1 W - \frac{\tilde{W}_c^T\bar{\sigma}}{m_\sigma}\varepsilon_H \\ -\tilde{W}_c^T A_1\tilde{W}_c - \tilde{W}_a^T A_2\tilde{W}_a + \tilde{W}_a^T A_3\tilde{W}_c + \tilde{W}_a^T B_1 + B_2\end{aligned} \tag{51}$$

Where

$$A_1 = \frac{1}{2}\bar{\sigma}\bar{\sigma}^T + \frac{\beta}{2}\Gamma^{-1}, A_2 = \frac{(\eta_{a1}+\eta_{a2})}{\eta_a}I - \frac{1}{4}D_1\frac{\bar{\sigma}^T}{m_\sigma}W$$
$$A_3 = \frac{1}{4}D_1 W\frac{\bar{\sigma}^T}{m_\sigma} + \frac{\eta_{a1}}{\eta_a}I$$
$$B_1 = \frac{1}{2}D_1 W + \frac{1}{2}\bigtriangledown\phi D_2 \bigtriangledown\varepsilon_\upsilon - \frac{1}{4}D_1 W\frac{\bar{\sigma}^T}{m_\sigma}W + \frac{\eta_{a2}}{\eta_a}W$$
$$B_2 = \gamma W^T\phi + \frac{1}{4}\bigtriangledown\varepsilon_\upsilon^T D_2 \bigtriangledown\varepsilon_\upsilon + \gamma\varepsilon_\upsilon(z)$$

The boundness ofε_υ and $\bigtriangledown\varepsilon_\upsilon$, positive constants $\kappa_1, \kappa_2, \kappa_3$ such that $||B_1|| \leq \kappa_1, ||B_2|| \leq \kappa_2$, $||(1/4)D_1(\bar{\sigma}^T/m_\sigma)W|| \leq \kappa_3$. Using the Young's inequality, (51) becomes

$$\begin{aligned}\dot{V}(t) \leq -\underline{q}||e||^2 - \frac{\beta}{4\alpha_2}||\tilde{W}_c||^2 - \frac{\eta_{a1}+\eta_{a2}}{2\eta_a}||\tilde{W}_a||^2 \\ - \left(\frac{\beta}{4\alpha_2} - \frac{1}{2\epsilon}\left(\frac{\eta_a 1}{\eta_a} + \kappa_3\right)\right)||\tilde{W}_c||^2 \\ - \left(\frac{\eta_{a1}+\eta_{a2}}{2\eta_a} - \kappa_3 - \frac{\epsilon}{2}\left(\frac{\eta_{a1}}{\eta_a} + \kappa_3\right)\right) \\ \times||\tilde{W}_a||^2 + \frac{\varepsilon_h}{\sqrt{\upsilon\alpha_1}}||\tilde{W}_c|| + \kappa_1||\tilde{W}_a|| + \kappa_2\end{aligned} \tag{52}$$

Where $\underline{q} = \lambda_{min}(Q)$. Choose $(\beta/4\alpha_2) \geq (1/2\epsilon)((\eta_{a1}/\eta_a) + \kappa_3)$ and $((\eta_{a1} + \eta_{a2}/2\eta_a) \geq \kappa_3 + (\epsilon/2)((\eta_{a1}/\eta_a) + \kappa_3)$ (52) becomes

$$\dot{V}(t) \leq -\bar{\omega}_1||\zeta||^2 + \bar{\omega}_2||\zeta|| + \kappa_2$$

Applying (41) and (43) gives

$$u^* - \hat{u} = -\frac{1}{2}R^{-1}G^T(\bigtriangledown\phi^T(z)\tilde{W}_a + \bigtriangledown\varepsilon_\upsilon)$$

According one can get

$$||u^* - \hat{u}|| \leq \frac{1}{2\lambda_{min}(R)}b_g(b_{\phi z}b_\zeta + b_{\varepsilon z}) = b_u \tag{53}$$

Where b_u is a positive constant Therefore, the tracking error dynamics of the FMWR (18) is eventually bounded uniformly, which further shows that the state $q(t)$ can track the desired trajectory $qr(t)$.

4. Simulation and Results

This section presents simulation-based validation of the proposed RISE-Based Actor–Critic Reinforcement Learning (RISE-AC RL) controller for a four-wheeled Mecanum mobile robot subject to center-of-mass (COM) offset and external uncertainties. All simulations are conducted in MATLAB/Simulink using a continuous-time plant model with numerical integration.

4.1. Robot Model and Simulation Setup

The robot is modeled as a planar 3-DOF system with generalized coordinates $q = [x,\ y,\ \phi]^T$ and four wheel torques $\tau = [\tau_1, \tau_2, \tau_3, \tau_4]^T$. The center-of-mass (COM) offset (R_{CX}, R_{Cy}) is incorporated into the inertia and coupling terms of the dynamic model, capturing payload-induced mass-eccentricity effects.

Unless otherwise stated, the following nominal parameters are used:

- Body mass: $m_b = 12$ kg; wheel mass: $m_w = 0.313$ kg.
- Geometry: $a = 0.2$ m, $b = 0.3$ m; wheel radius: $r = 0.0508$ m.
- Body inertia: $I = 0.5\ \mathrm{kg\,m^2}$; wheel inertia: $I_w = 4.0378 \times 10^{-4}\ \mathrm{kg\,m^2}$.
- Gravitational acceleration: $g = 9.8\ \mathrm{m/s^2}$.

The initial state is selected to be significantly displaced from the reference trajectory:

$$\left[x(0),\, y(0),\, \phi(0),\, \dot{x}(0),\, \dot{y}(0),\, \dot{\phi}(0)\right]^T = \left[1.5,\, 1.5,\, 1.4,\, 0,\, 0,\, 0\right]^T. \tag{54}$$

The total simulation duration is $T = 50$ s. The control update period is set to $\Delta t \in [1, 5]$ ms (depending on the solver configuration) to accurately capture online learning transients and the RISE compensation dynamics.

The controller parameters were set to comparable levels, as summarized in Table 1, to ensure a fair evaluation of the proposed controller.

4.2. Simulation Cases

4.2.1. Case 1: Baseline Evaluation Under Slippage and Fixed Com Offset

This case is designed as a baseline test to evaluate the trajectory-tracking performance of the proposed controller under wheel–ground slippage and a constant center-of-mass (COM) offset. A time-varying slippage profile $\rho(t)$ is imposed, while the COM offset is fixed at

$$r_x = r_y = 0.15\ \mathrm{m}. \tag{55}$$

No external disturbance torque is applied, i.e., $\tau_d(t) = 0$, and the payload variation is neglected. Under this condition, the tracking degradation is mainly caused by slippage and static mass eccentricity.

Table 1. Parameter settings for each controller

Methodology	Parameters	Values
Robust-based RL [38]	$R,\ Q,\ \gamma,\ \eta_c,\ \eta_{a1},\ \eta_{a2}$ $\beta,\ \nu,\ \eta_a$	$I_3,\ 10I_6,\ 10^{-3},\ 2.3,\ 8,\ 10^{-3}$ $10^{-3},\ 10^{-3},\ 10^{-3}$
RISE-AC RL	$R,\ Q,\ \gamma,\ \eta_c,\ \eta_{a1},\ \eta_{a2}$ $\beta,\ \nu,\ \lambda_1,\ \lambda_2,\ \beta_1,\ k_s$	$I_3,\ 10I_6,\ 0.5,\ 0.08,\ 0.2,\ 50$ $10^{-3},\ 10^{-3},\ 4I_3,\ 50,\ 6,\ 100$

As shown in Fig. 3, both the robust-based RL controller and the proposed RISE-AC RL controller converge from the large initial displacement to the circular reference trajectory under wheel slippage and a fixed center-of-mass (COM) offset. This result confirms that both controllers are able to maintain stable trajectory tracking in the presence of static mass eccentricity and slip-induced uncertainty. Nevertheless, the zoomed view in Fig. 3 shows that the proposed RISE-AC RL controller remains closer to the reference trajectory and exhibits a smaller steady-state bias than the robust-based RL baseline, indicating improved tracking accuracy under the considered operating condition.

The tracking errors in Fig. 4(a) decrease rapidly during the initial transient and then remain within a small neighborhood around zero under wheel slippage and a fixed center-of-mass (COM) offset. Compared with the robust-based RL controller, the proposed RISE-AC RL controller yields smaller residual errors in both the translational and heading channels, indicating improved steady-state tracking accuracy in the presence of static mass eccentricity and slip-induced uncertainty. In addition, the wheel torque commands of the proposed controller in Fig. 4(b) remain bounded and gradually evolve into smooth periodic signals after a short transient, which is consistent with the steady circular motion of the robot.

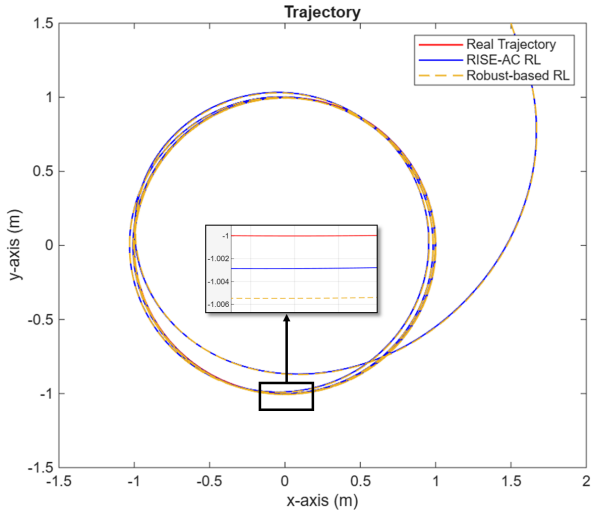

Fig. 3. Tracking trajectory: robust-based RL and RISE-AC RL

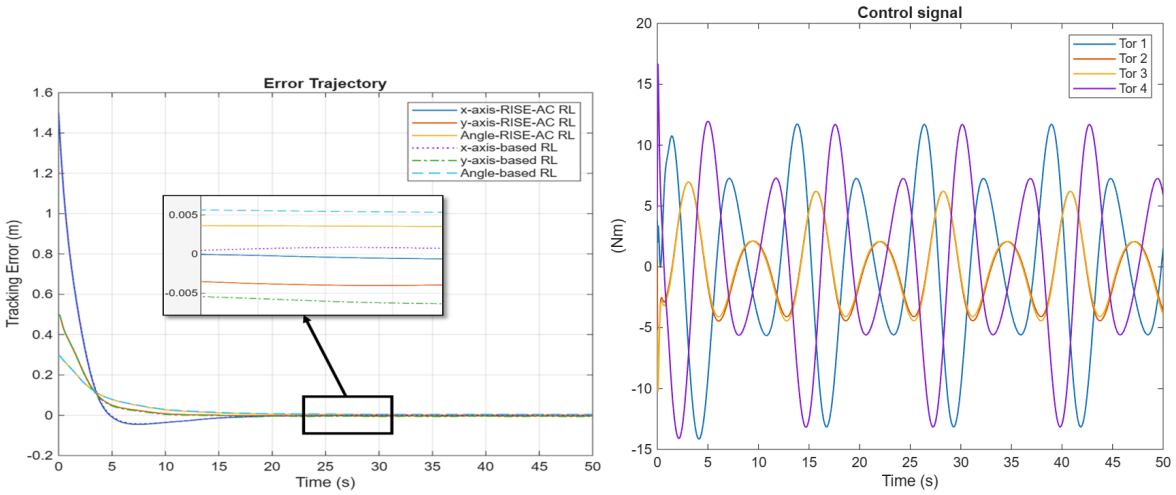

(a) **(b)**

Fig. 4. (a) The tracking error. (b) Control signal RISE–AC RL

Finally, Fig. 5 shows that the critic and actor weights (W_c and W_a) adapt rapidly during the transient phase and then gradually converge to stable values, indicating a well-behaved online learning process under wheel slippage and a fixed center-of-mass (COM) offset. These results further confirm that the proposed RISE-AC RL framework preserves stable weight adaptation and improves steady-state tracking performance while maintaining bounded control effort in the presence of static mass eccentricity and slip-induced uncertainty.

4.2.2. Case 2: Combined-Uncertainty Robustness Test (Slippage, COM Offset, Payload Variation, and Disturbances)

To evaluate the effectiveness and robustness of the proposed control strategy, numerical simulations are conducted on a four-wheeled Mecanum mobile robot under concurrent and strongly time-varying uncertainties that closely reflect practical operating conditions. Specifically, the robot is subjected simultaneously to a time-varying slippage profile, a nonzero center-of-mass (COM) offset (r_x, r_y), payload variation Δm, and external disturbance torques $\tau_d(t)$.

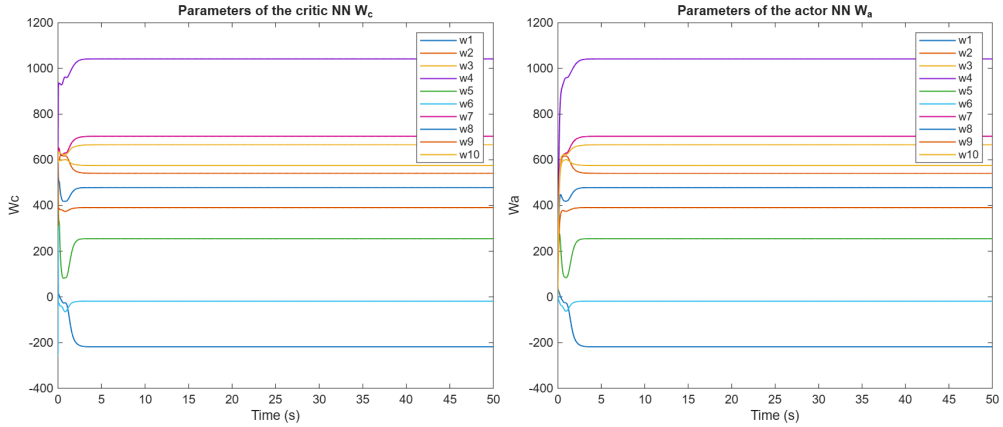

Fig. 5. Weights of the critic and the actor networks RISE–AC RL

The CoM offset is assumed to vary according to the following time-dependent functions:

$$\begin{aligned} r_x(t) &= 0.05\sin(0.8t) + 0.025\cos(1.5t) + 0.03\sin(2.5t), \\ r_y(t) &= 0.03\sin(0.3t) + 0.06\cos(1.2t) + 0.05\sin(2.8t) + 0.02\cos(3.5t), \end{aligned} \tag{44}$$

Where r_x and dr_y denote the COM offsets along the x- and y-axes, respectively. In addition, the robot mass is assumed to vary with an amplitude of

$$\Delta m = 3 \text{ kg}. \tag{56}$$

The Gaussian noise signal is implemented numerically as

$$\varepsilon_{\text{Gauss}} = \text{normrnd}(0,\ 1.5,\ \text{size}(t)). \tag{57}$$

As shown in Fig. 6, the COM undergoes continuous variations, which strengthen translation–rotation coupling and induce wheel-dependent traction changes, making the tracking problem more challenging than in Case 1.

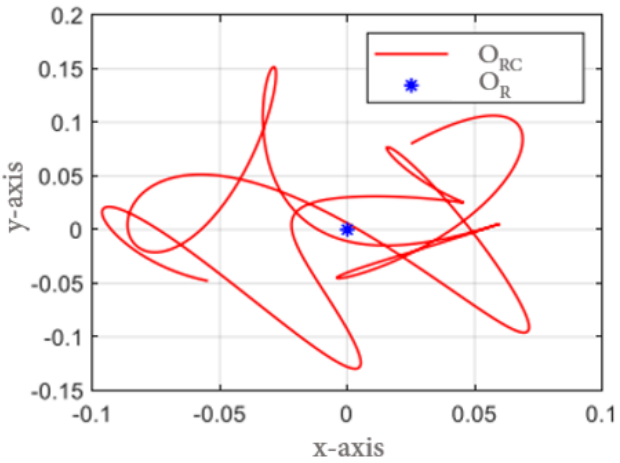

Fig. 6. Time-varying trajectory of the robot center of mass relative to its nominal position

Fig. 6 illustrates the time–varying trajectory of the robot's center of mass relative to its nominal position. The tracking trajectories in Fig. 7 show that both controllers can follow the reference path,

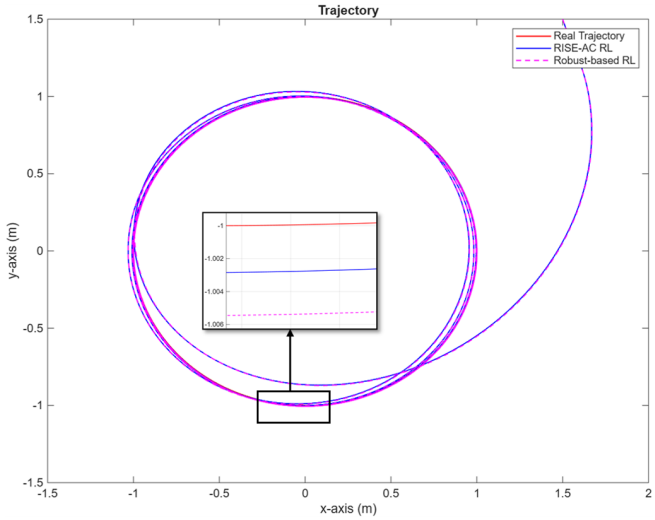

Fig. 7. Simulated trajectory tracking performance of the robot under external disturbances and center-of-mass (COM) offset

While robust-based RL exhibits larger deviations on several segments. In contrast, the proposed RISE-AC RL stays closer to the real trajectory with reduced steady-state bias, owing to the RISE disturbance compensation and the online actor–critic policy update with a discounted cost. The simulation results of the trajectory tracking errors in Fig. 8a and the RMSE comparison of trajectory tracking errors in Fig. 8b show that the proposed RISE-AC RL algorithm achieves better trajectory tracking performance than the RISE-based RL algorithm. Specifically, the proposed controller yields smaller tracking errors and lower RMSE values, thereby demonstrating its improved tracking accuracy.

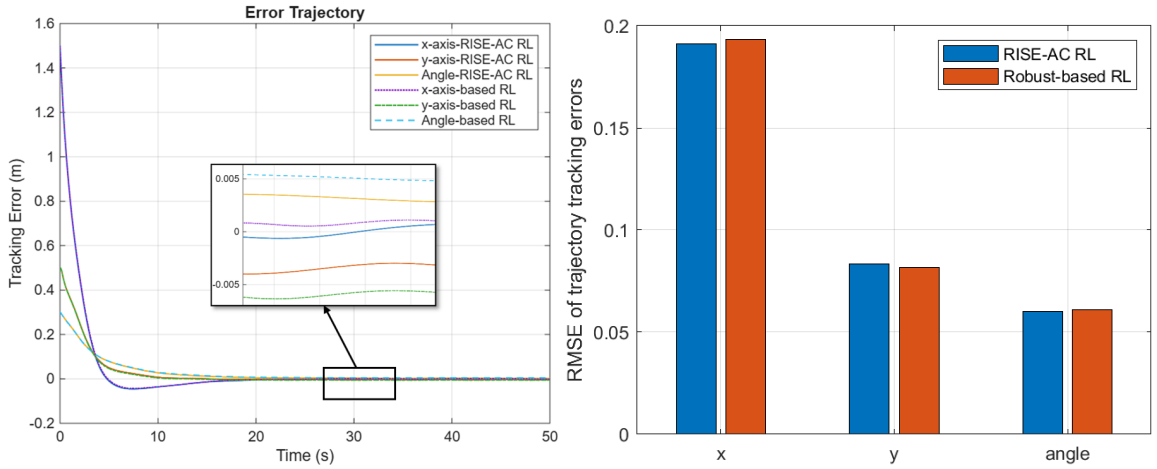

(a) **(b)**

Fig. 8. (a) Trajectory tracking errors under external disturbances and center-of-mass (COM) offset. (b) RMSE comparison of trajectory tracking errors between the proposed RISE-AC RL and the Robust-based RL

The simulation results in Fig. 10 show that the proposed RISE-based RL controller requires a lower total control input than the Robust-based RL controller. Specifically, the performance index H, which reflects the control effort and the associated energy-related consumption, is reduced from $1392(N.m.s)$ for the Robust-based RL method to $1289(N.m.s)$ for the proposed RISE-based RL controller. This result indicates that the proposed method is more energy-efficient. As shown in Fig. 9,

both the Actor and Critic neural network weights converge at approximately 6 s, which confirms the stability and learning effectiveness of the proposed algorithm under a time-varying center-of-mass offset condition.

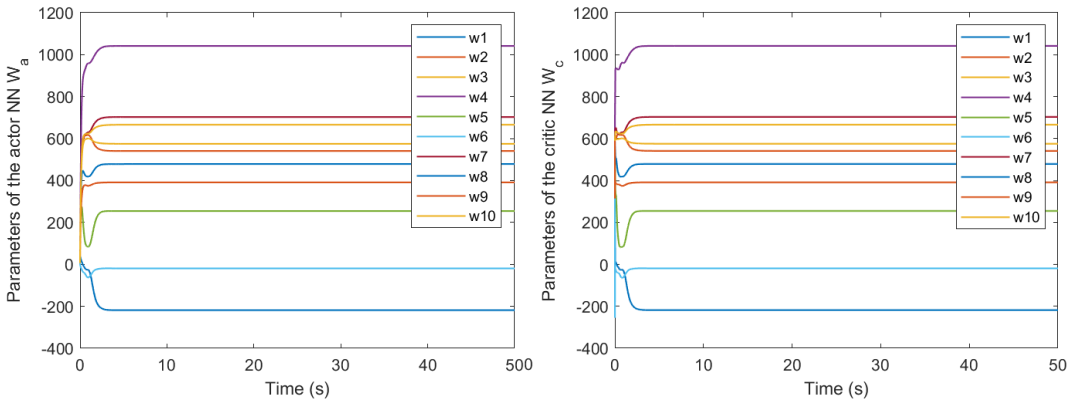

Fig. 9. Evolution of the actor $\hat{W}_a$ and critic $\hat{W}_c$ neural network weights under a time-varying center-of-mass offset

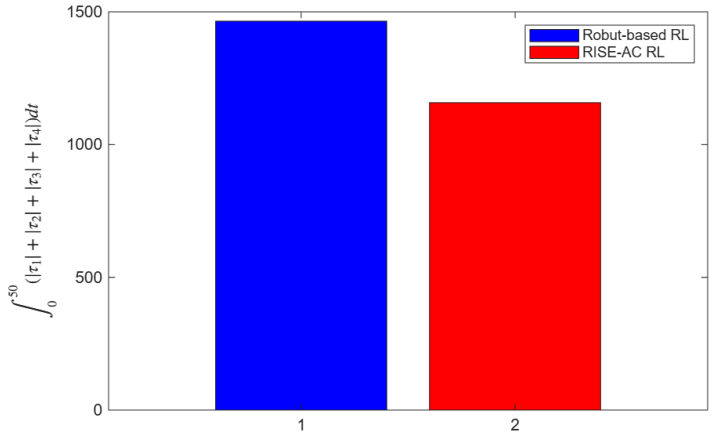

Fig. 10. Comparison of nominal energy consumption for each method

5. Conclusion

This paper proposed a RISE-based Actor–Critic reinforcement learning controller for trajectory tracking of a four-wheeled Mecanum mobile robot under center-of-mass (COM) offset and dynamic uncertainties. By integrating the online Actor–Critic learning mechanism with the RISE compensation term, the proposed method improved tracking accuracy and robustness against slip-related disturbances, payload-induced mass eccentricity, and disturbances caused by the center-of-mass offset. Simulation results under both fixed and time-varying uncertainty conditions showed that the proposed RISE-AC RL controller achieved smaller tracking errors, lower RMSE values, and reduced control effort than the robust-based RL controller, while maintaining stable convergence of the actor and critic neural network weights. These results confirm the effectiveness of the proposed method for trajectory tracking of Mecanum mobile robots under COM-offset and uncertainty conditions, and future work will focus on experimental validation and extension to more challenging robotic operating scenarios.

Author Contribution: All authors contributed equally to the main contributor to this paper. All authors read and approved the final paper.

Funding: This research received no external funding.

Conflicts of Interest: The authors declare no conflict of interest.

References

[1] S. S. Alatyrev, R. V. Andreev, A. O. Vasiliev, N. N. Pushkarenko, A. O. Grigoryev and S. V. Tikhonov, "Influence of the parameters of support wheels on the amount of the device of the trailer from the tracking course," *IOP Conference Series: Materials Science and Engineering*, vol. 457, p. 012002, 2018, https://doi.org/10.1088/1757-899X/457/1/012002.

[2] G. Campion, G. Bastin and B. Dandrea-Novel, "Structural properties and classification of kinematic and dynamic models of wheeled mobile robots," in *IEEE Transactions on Robotics and Automation*, vol. 12, no. 1, pp. 47-62, 1996, https://doi.org/10.1109/70.481750.

[3] H. Xing, Y. Xu, L. Ding, J. Chen, H. Gao and M. Tavakoli, "Trajectory Tracking Control of Wheeled Mobile Manipulators With Joint Flexibility via Virtual Decomposition Approach," in *IEEE Transactions on Automation Science and Engineering*, vol. 22, pp. 11808-11825, 2025, https://doi.org/10.1109/TASE.2025.3540860.

[4] Y. Yamamoto and Xiaoping Yun, "Modeling and compensation of the dynamic interaction of a mobile manipulator," *Proceedings of the 1994 IEEE International Conference on Robotics and Automation*, vol. 3, pp. 2187-2192, 1994, https://doi.org/10.1109/ROBOT.1994.350960.

[5] K. M. Lynch and F. C. Park, *Modern robotics*, Cambridge University Press, 2017, https://books.google.co.id/books?id=5NzFDgAAQBAJ&hl=id&source=gbs_navlinks_s.

[6] I. Zeidis and K. Zimmermann, "Dynamics of a four-wheeled mobile robot with Mecanum wheels," *ZAMM-Journal of Applied Mathematics and Mechanics/Zeitschrift für Angewandte Mathematik und Mechanik*, vol. 99, no. 12, p. e201900173, 2019, https://doi.org/10.1002/zamm.201900173

[7] H. Taheri, B. Qiao and N. Ghaeminezhad, "Kinematic model of a four mecanum wheeled mobile robot," *International journal of computer applications*, vol. 113, no. 3, pp. 6-9, 2015, https://doi.org/10.5120/19804-1586.

[8] M. Abdelrahman, I. Zeidis, O. Bondarev, B. Adamov, F. Becker, and K. Zimmermann, "A description of the dynamics of a four-wheel Mecanum mobile system as a basis for a platform concept for special purpose vehicles for disabled persons," *58th Ilmenau Scientific Colloquium Technische Universität Ilmenau*, pp. 1–10, 2014, https://www.db-thueringen.de/servlets/MCRFileNodeServlet/dbt_derivate_00030822/ilm1-2014iwk-041.pdf.

[9] N. Tlale and M. de Villiers, "Kinematics and Dynamics Modelling of a Mecanum Wheeled Mobile Platform," *2008 15th International Conference on Mechatronics and Machine Vision in Practice*, pp. 657-662, 2008, https://doi.org/10.1109/MMVIP.2008.4749608.

[10] L. -C. Lin and H. -Y. Shih, "Modeling and adaptive control of an omni-mecanum-wheeled robot," *Department of Mechanical Engineering, National Chung Hsing University*, vol. 4, no. 2, pp. 166–179, 2013, https://doi.org/10.4236/ica.2013.42021.

[11] F. Becker, O. Bondarev, I. Zeidis and K. Zimmermann, "An approach to the kinematics and dynamics of a four-wheel Mecanum vehicle," *Scientific Journal of Iftomm "Problems of Mechanics"*, vol. 55, pp. 27–37, 2014, https://istina.msu.ru/media/publications/article/7fc/698/21059172/an-approach-to-the-kinematics-and-dynamics-of-a-four-wheel-mecanum-vehicle.pdf.

[12] V. Padois, J. -Y. Fourquet and P. Chiron, "Kinematic and dynamic model-based control of wheeled mobile manipulators: A unified framework for reactive approaches," *Robotica*, vol. 25, no. 2, pp. 157–173, 2007, https://doi.org/10.1017/S0263574707003360.

[13] Y. Yamamoto and Xiaoping Yun, "Modeling and compensation of the dynamic interaction of a mobile manipulator," *Proceedings of the 1994 IEEE International Conference on Robotics and Automation*, vol. 3, pp. 2187-2192, 1994, https://doi.org/10.1109/ROBOT.1994.350960.

[14] I. Zeidis and K. Zimmermann, "Dynamics of a four-wheeled mobile robot with Mecanum wheels," *ZAMM-Journal of Applied Mathematics and Mechanics/Zeitschrift für Angewandte Mathematik und Mechanik*, vol. 99, no. 12, p. e201900173, 2019, https://doi.org/10.1002/zamm.201900173.

[15] H. Taheri B. Qiao and N. Ghaeminezhad, "Kinematic model of a four mecanum wheeled mobile robot," *International journal of computer applications*, vol. 113, no. 3, pp. 6-9, 2015, https://doi.org/10.5120/19804-1586.

[16] M. Abdelrahman, I. Zeidis, O. Bondarev, B. Adamov, F. Becker, and K. Zimmermann, "A description of the dynamics of a four-wheel Mecanum mobile system as a basis for a platform concept for special purpose vehicles for disabled persons," *58th ilmenau scientific colloquium technische universität ilmenau*, pp. 1–10, 2014, https://www.db-thueringen.de/servlets/MCRFileNodeServlet/dbt_derivate_00030822/ilm1-2014iwk-041.pdf.

[17] N. Tlale and M. de Villiers, "Kinematics and Dynamics Modelling of a Mecanum Wheeled Mobile Platform," *2008 15th International Conference on Mechatronics and Machine Vision in Practice*, pp. 657-662, 2008, https://doi.org/10.1109/MMVIP.2008.4749608.

[18] F. Becker, O. Bondarev, I. Zeidis, K. Zimmermann, M. Abdelrahman and B. Adamov, "An approach to the kinematics and dynamics of a four-wheel Mecanum vehicle," *scientific journal of iftomm "problems of mechanics"*, vol. 2, no. 55, pp. 27–37, 2014, https://istina.msu.ru/media/publications/article/7fc/698/21059172/an-approach-to-the-kinematics-and-dynamics-of-a-four-wheel-mecanum-vehicle.pdf.

[19] P. Wu, K. Wang, J. Zhang and Q. Zhang, "Optimal design for pid controller based on de algorithm in omnidirectional mobile robot," In *MATEC Web of Conferences*, vol. 95, no. 08014, 2017, https://doi.org/10.1051/matecconf/20179508014.

[20] S. Khorshidi, M. Dawood and M. Bennewitz, "Centroidal State Estimation Based on the Koopman Embedding for Dynamic Legged Locomotion," *2024 IEEE/RSJ International Conference on Intelligent Robots and Systems (IROS)*, pp. 12832-12839, 2024, https://doi.org/10.1109/IROS58592.2024.10801750.

[21] V. Padois, J.-Y. Fourquet and P. Chiron, "Kinematic and Dynamic Model-Based Control of Wheeled Mobile Manipulators: A Unified Framework for Reactive Approaches," *Robotica*, vol. 25, no. 2, pp. 157–73, https://doi.org/10.1017/S0263574707003360.

[22] J. C. O. Hernández and D. I. R. Almeida, "Experimental control approach of a mecanum-wheeled mobile robot for slippage error and energy consumption reduction on different surfaces," *Journal of Mechanical Science and Technology*, vol. 38, pp. 6309–6318, 2024, https://doi.org/10.1007/s12206-024-1042-8.

[23] Z. Sun, S. Hu, D. He, W. Zhu, H. Xie and J. Zhang, "Trajectory-tracking control of Mecanum-wheeled omnidirectional mobile robots using adaptive integral terminal sliding mode," *ACM Digital Library*, vol. 96, 2021, https://doi.org/10.1016/j.compeleceng.2021.107500.

[24] Y. Liu, J. M. Zhu, R. L. Williams and J. Wu, "Omni-directional mobile robot controller based on trajectory linearization," *Robotics and autonomous systems*, vol. 56, no. 5, pp. 461-479, 2008, http://dx.doi.org/10.1016/j.robot.2007.08.007.

[25] Z. Hendzel and M. Ko lodziej, "Robust tracking control of omni-Mecanum wheeled robot," *Automation 2021: Recent Achievements in Automation, Robotics and Measurement Techniques*, vol. 1390, pp. 219–229, 2021, https://doi.org/10.1007/978-3-030-74893-7_21.

[26] R. Solea, A. Filipescu and U. Nunes, "Sliding-mode control for trajectory-tracking of a Wheeled Mobile Robot in presence of uncertainties," *2009 7th Asian Control Conference*, pp. 1701-1706, 2009, https://ieeexplore.ieee.org/abstract/document/5276210.

[27] J. J. E. Slotine and W. Li, *Applied nonlinear control*, Prentice Hall, 1991, https://www.academia.edu/download/59109257/01-Applied_Nonlinear_Control20190502-126300-11lqjz5.pdf.

[28] K. G. Vamvoudakis, "An online actor/critic algorithm for event-triggered optimal control of continuous-time nonlinear systems," *2014 American Control Conference, Portland*, pp. 1-6, 2014, https://doi.org/10.1109/ACC.2014.6859198.

[29] B. Kiumarsi, K. G. Vamvoudakis, H. Modares and F. L. Lewis, "Optimal and Autonomous Control Using Reinforcement Learning: A Survey," in *IEEE Transactions on Neural Networks and Learning Systems*, vol. 29, no. 6, pp. 2042-2062, 2018, https://doi.org/10.1109/TNNLS.2017.2773458.

[30] F. L. Lewis and D. Liu, *Reinforcement learning and approximate dynamic programming for feedback control*, John Wiley & Sons, 2013, https://books.google.co.id/books?id=wH4Uy-ZFluwC&hl=id&source=gbs_navlinks_s.

[31] D. Lee, J. Byun and H. J. Kim, "RISE-Based Trajectory Tracking Control of an Aerial Manipulator Under Uncertainty," in *IEEE Control Systems Letters*, vol. 6, pp. 3379-3384, 2022, https://doi.org/10.1109/LCSYS.2022.3184820.

[32] S. Shao and K. Zhang, "RISE-Adaptive Neural Control for Robotic Manipulators With Unknown Disturbances," in *IEEE Access*, vol. 8, pp. 97729-97736, 2020, https://doi.org/10.1109/ACCESS.2020.2997383.

[33] B. Xian, D. M. Dawson, M. S. de Queiroz and J. Chen, "A continuous asymptotic tracking control strategy for uncertain nonlinear systems," in *IEEE Transactions on Automatic Control*, vol. 49, no. 7, pp. 1206-1211, 2004, https://doi.org/10.1109/TAC.2004.831148.

[34] N. Fischer, Z. Kan, R. Kamalapurkar and W. E. Dixon, "Saturated RISE Feedback Control for a Class of Second-Order Nonlinear Systems," in *IEEE Transactions on Automatic Control*, vol. 59, no. 4, pp. 1094-1099, 2014, https://doi.org/10.1109/TAC.2013.2286913.

[35] H. J. Asl, T. Narikiyo, and M. Kawanishi, "RISE-based prescribed performance control of Euler–Lagrange systems," *Journal of the Franklin Institute*, vol. 356, no. 13, pp. 7144-7163, 2019, https://doi.org/10.1016/j.jfranklin.2019.06.033.

[36] L. C. Lin and H. -Y. Shih, "Modeling and adaptive control of an omni-mecanum-wheeled robot," *Intelligent Control and Automation*, vol. 4, pp. 166–179, 2013, http://dx.doi.org/10.4236/ica.2013.42021.

[37] C. S. Shijin and K. Udayakumar, "Speed control of wheeled mobile robots using PID with dynamic and kinematic modelling," *2017 International Conference on Innovations in Information, Embedded and Communication Systems (ICIIECS)*, pp. 1-7, 2017, https://doi.org/10.1109/ICIIECS.2017.8275962.

[38] M. D. Nguyen, M. T. Ngo, H. D. Quang and N. D. Phuong, "Reinforcement Learning-Based Trajectory Control for Mecanum Robot with Mass Eccentricity Considerations," *Journal of Robotics and Control*, vol. 5, no. 5, pp. 1436–1443, 2024, https://doi.org/10.18196/jrc.v5i5.22148.

[39] R. Solea, A. Filipescu and U. Nunes, "Sliding-mode control for trajectory-tracking of a Wheeled Mobile Robot in presence of uncertainties," *2009 7th Asian Control Conference*, pp. 1701-1706, 2009, https://ieeexplore.ieee.org/abstract/document/5276210.

[40] P. Mehta and S. Meyn, "Q-learning and Pontryagin's Minimum Principle," *Proceedings of the 48h IEEE Conference on Decision and Control (CDC) held jointly with 2009 28th Chinese Control Conference*, pp. 3598-3605, 2009, https://doi.org/10.1109/CDC.2009.5399753.

[41] K. G. Vamvoudakis and F. L. Lewis, "Online actor–critic algorithm to solve the continuous-time infinite horizon optimal control problem," *Automatica*, vol. 46, no. 5, pp. 878-888, 2010, https://doi.org/10.1016/j.automatica.2010.02.018.

[42] H. Zhang, L. Cui, X. Zhang and Y. Luo, "Data-Driven Robust Approximate Optimal Tracking Control for Unknown General Nonlinear Systems Using Adaptive Dynamic Programming Method," in *IEEE Transactions on Neural Networks*, vol. 22, no. 12, pp. 2226-2236, 2011, https://doi.org/10.1109/TNN.2011.2168538.

[43] S. Bhasin, R. Kamalapurkar, M. Johnson, K. G. Vamvoudakis, F. L. Lewis, W. E. Dixon, "A novel actor–critic–identifier architecture for approximate optimal control of uncertain nonlinear systems," *Automatica*, vol. 49, no. 1, pp. 82-92, 2013, https://doi.org/10.1016/j.automatica.2012.09.019.

[44] K. Dupree, P. M. Patre, Z. D. Wilcox and W. E. Dixon, "Asymptotic optimal control of uncertain nonlinear Euler–Lagrange systems," *Automatica*, vol. 47, no. 1, pp. 99-107, 2011, https://doi.org/10.1016/j.automatica.2010.10.007.

[45] D. Zhang, G. Wang and Z. Wu, "Reinforcement Learning-Based Tracking Control for a Three Mecanum Wheeled Mobile Robot," in *IEEE Transactions on Neural Networks and Learning Systems*, vol. 35, no. 1, pp. 1445-1452, 2024, https://doi.org/10.1109/TNNLS.2022.3185055.

[46] Z. Feng and J. Fei, "Super-Twisting Sliding Mode Control for Micro Gyroscope Based on RBF Neural Network," in *IEEE Access*, vol. 6, pp. 64993-65001, 2018, https://doi.org/10.1109/ACCESS.2018.2877398.

[47] W. Lin, X. Huo, Z. Jin, B. Wu and Z. Liu, "Sliding Mode Control of Manipulator Based on Nominal Model and Nonlinear Disturbance Observer," *IECON 2018 - 44th Annual Conference of the IEEE Industrial Electronics Society*, pp. 5519-5524, 2018, https://doi.org/10.1109/IECON.2018.8592926.

[48] Y. Pan, X. Li, H. Wang and H. Yu, "Continuous sliding mode control of compliant robot arms: A singularly perturbed approach," *Mechatronics*, vol. 52, pp. 127-134, 2018, https://doi.org/10.1016/j.mechatronics.2018.04.005.

[49] K. Bai, X. Gong, S. Chen, Y. Wang and Z. Liu, "Sliding mode nonlinear disturbance observer-based adaptive back-stepping control of a humanoid robotic dual manipulator" *Robotica*, vol. 36, no. 11, pp. 1728-1742, 2018, https://doi.org/10.1017/S026357471800067X.

[50] J. Kim and I. Yang, "Hamilton-Jacobi-Bellman equations for Q-learning in continuous time," *Proceedings of the 2nd Conference on Learning for Dynamics and Control*, vol. 120, pp. 739-748, 2020, https://proceedings.mlr.press/v120/kim20b.html.

[51] B. Luo, H. -N. Wu, T. Huang and D. Liu, "Reinforcement learning solution for HJB equation arising in constrained optimal control problem," *Neural Networks*, vol. 71, pp. 150-158, 2015, https://doi.org/10.1016/j.neunet.2015.08.007.

[52] H. E. Wiltzer, D. Meger and M. G. Bellemare, "Distributional hamilton-jacobi-bellman equations for continuous-time reinforcement learning," *Proceedings of the 39th International Conference on Machine Learning*, vol. 16, pp. 23832-23856, 2022, https://proceedings.mlr.press/v162/wiltzer22a.html.

[53] J. W. Kim, B. J. Park, H. Yoo, T. Hoon Oh, J. H. Lee and J. M. Lee, "A model-based deep reinforcement learning method applied to finite-horizon optimal control of nonlinear control-affine system," *Journal of Process Control*, vol. 87, pp. 166-178, 2020, https://doi.org/10.1016/j.jprocont.2020.02.003.

[54] W. Xiao, Q. Zhou, Y. Liu, H. Li and R. Lu, "Distributed Reinforcement Learning Containment Control for Multiple Nonholonomic Mobile Robots," in *IEEE Transactions on Circuits and Systems I: Regular Papers*, vol. 69, no. 2, pp. 896-907, 2022, https://doi.org/10.1109/TCSI.2021.3121809.

[55] K. G. Vamvoudakis, "An online actor/critic algorithm for event-triggered optimal control of continuous-time nonlinear systems," *2014 American Control Conference*, pp. 1-6, 2014, https://doi.org/10.1109/ACC.2014.6859198.

[56] B. Kiumarsi, K. G. Vamvoudakis, H. Modares and F. L. Lewis, "Optimal and Autonomous Control Using Reinforcement Learning: A Survey," in *IEEE Transactions on Neural Networks and Learning Systems*, vol. 29, no. 6, pp. 2042-2062, 2018, https://doi.org/10.1109/TNNLS.2017.2773458.

[57] F. L. Lewis and D. Liu, *Reinforcement Learning and Approximate Dynamic Programming for Feedback Control*, John Wiley & Sons, 2013, https://books.google.co.id/books?id=wH4Uy-ZFluwC&hl=id&source=gbs_navlinks_s.

[58] D. Lee, J. Byun and H. J. Kim, "RISE-Based Trajectory Tracking Control of an Aerial Manipulator Under Uncertainty," in *IEEE Control Systems Letters*, vol. 6, pp. 3379-3384, 2022, https://doi.org/10.1109/LCSYS.2022.3184820.

[59] S. Shao and K. Zhang, "RISE-Adaptive Neural Control for Robotic Manipulators With Unknown Disturbances," in *IEEE Access*, vol. 8, pp. 97729-97736, 2020, https://doi.org/10.1109/ACCESS.2020.2997383.

[60] B. Xian, D. M. Dawson, M. S. de Queiroz and J. Chen, "A continuous asymptotic tracking control strategy for uncertain nonlinear systems," in *IEEE Transactions on Automatic Control*, vol. 49, no. 7, pp. 1206-1211, 2004, https://doi.org/10.1109/TAC.2004.831148.

[61] N. Fischer, Z. Kan, R. Kamalapurkar and W. E. Dixon, "Saturated RISE Feedback Control for a Class of Second-Order Nonlinear Systems," in *IEEE Transactions on Automatic Control*, vol. 59, no. 4, pp. 1094-1099, 2014, https://doi.org/10.1109/TAC.2013.2286913.

[62] H. J. Asl, T. Narikiyo and M. Kawanishi, "RISE-based prescribed performance control of Euler–Lagrange systems," *Journal of the Franklin Institute*, vol. 356, no. 13, pp. 7144–7163, 2019, https://doi.org/10.1016/j.jfranklin.2019.06.033.